LDL particle core enrichment in cholesteryl oleate increases proteoglycan binding and promotes atherosclerosis[S]

John T. Melchior,* Janet K. Sawyer,* Kathryn L. Kelley,* Ramesh Shah,* Martha D. Wilson,* Roy R. Hantgan,[†] and Lawrence L. Rudel*,[†]

Department of Pathology, Section of Lipid Sciences,* and Department of Biochemistry,[†] Wake Forest University School of Medicine, Winston Salem, NC

Abstract **Several studies in humans and animals suggest that LDL particle core enrichment in cholesteryl oleate (CO) is associated with increased atherosclerosis. Diet enrichment with MUFAs enhances LDL CO content. Steroyl *O*-acyltransferase 2 (SOAT2) is the enzyme that catalyzes the synthesis of much of the CO found in LDL, and gene deletion of SOAT2 minimizes CO in LDL and protects against atherosclerosis. The purpose of this study was to test the hypothesis that the increased atherosclerosis associated with LDL core enrichment in CO results from an increased affinity of the LDL particle for arterial proteoglycans. ApoB-100-only *Ldlr*$^{-/-}$ mice with and without *Soat2* gene deletions were fed diets enriched in either *cis*-MUFA or n-3 PUFA, and LDL particles were isolated. LDL:proteogylcan binding was measured using surface plasmon resonance. Particles with higher CO content consistently bound with higher affinity to human biglycan and the amount of binding was shown to be proportional to the extent of atherosclerosis of the LDL donor mice. The data strongly support the thesis that atherosclerosis was induced through enhanced proteoglycan binding of LDL resulting from LDL core CO enrichment.—** Melchior, J. T., J. K. Sawyer, K. L. Kelley, R. Shah, M. D. Wilson, R. R. Hantgan, and L. L. Rudel. **LDL particle core enrichment in cholesteryl oleate increases proteoglycan binding and promotes atherosclerosis. *J. Lipid Res.* 2013.** 54: **2495–2503.**

Supplementary key words lipoprotein • fatty acid • glycosaminoglycan• cholesterol

Atherosclerosis is the disease process in the artery wall leading to clinical complications of coronary heart disease, a disease that has cost more lives in the United States over the past century than the next four diseases combined (1). The subendothelial retention and accumulation of LDL in the artery wall is now recognized as an initiating event in the pathophysiology of atherosclerosis (2). After LDL particles enter the intima of the artery wall, they can interact with proteoglycans, which are structural proteins residing in the extracellular matrix that consist of one or more glycosaminoglycan (GAG) side-chains attached to core proteins. The LDL-proteoglycan complex is generally regarded as an electrostatic interaction (3). The sulfation pattern of the acidic sugar groups that form the GAG chains on the proteoglycans results in an overall negative charge that can interact with clusters of positively charged amino acid residues on apoB-100, the primary apolipoprotein present on the LDL particle (4). A proteoglycan frequently deposited in atherosclerotic plaques of humans (5, 6) and mice is biglycan (BGN) (7).

While plasma LDL cholesterol concentrations are predictive of the extent of atherosclerosis, LDL particles are heterogeneous in size and composition, and this heterogeneity may provide additional useful information about the role of LDL in atherosclerosis. For instance, studies have shown that diet-induced alterations in the FA composition of LDL core cholesteryl esters (CEs) can influence the atherogenic potential of LDL particles (8–11). In nonhuman primates, consumption of dietary MUFAs resulted in LDL particles containing a CE core enriched in cholesterol oleate (CO), which were positively associated with coronary artery atherosclerosis ($r = 0.8$) (10, 11). Importantly, a similar diet-related shift in the CE FA composition of LDL has been observed in humans in which consumption of oleate-enriched diets resulted in elevations in the percentage of CO in the LDL CE (12). Additionally, the large Atherosclerosis Risk in Communities Study revealed a

This work was supported by National Institutes of Health program, project Grant 1-PO1-HL-49373 (L.L.R., Principal Investigator) and Institutional Development Grant 2006-IDG-1004 from the North Carolina Biotechnology Center (R.R.H.).

Manuscript received 30 April 2013 and in revised form 5 June 2013.

Published, JLR Papers in Press, June 26, 2013
DOI 10.1194/jlr.M039644

Abbreviations: BGN, biglycan; CE, cholesteryl ester; CO, cholesteryl oleate; CS, chondroitin sulfate; DLS, dynamic light scattering; FC, free cholesterol; GAG, glycosaminoglycan; PL, phospholipid; RT, room temperature; RU, response unit; SOAT2, steroyl *O*-acyltransferase 2; SPR, surface plasmon resonance; TC, total cholesterol; TG, triglyceride; TPC, total plasma cholesterol; UC, ultracentrifugation.

To whom correspondence should be addressed.
e-mail: lrudel@wakehealth.edu

[S] The online version of this article (available at http://www.jlr.org) contains supplementary data in the form of four figures.

significant positive association between the percentage of plasma CE as CO and carotid artery intima-media thickness in patients with preclinical atherosclerosis (13).

Steroyl *O*-acyltransferase 2 (SOAT2) is a membrane-bound enzyme localized to the endoplasmic reticulum in hepatocytes and enterocytes that is at least partially responsible for the incorporation of CO into apoB-containing lipoproteins (14). Gene deletion of *Soat2* in mouse models has been shown to protect against LDL CO enrichment and the development of atherosclerosis, supporting the claim that inhibition of CO production is a viable therapeutic target in the treatment of disease (8, 15). Although evidence consistently implicates CO as an important component in the development of atherosclerosis, the mechanism by which it promotes accelerated disease development has remained elusive. The primary goal of this study was to establish whether LDL particle core enrichment with CO enhances interactions between the LDL particle and resident arterial proteoglycans, which could accelerate the development of atherosclerosis via increased LDL particle retention. To accomplish this goal, we developed a novel assay using surface plasmon resonance (SPR) technology to quantify the interaction of LDL particles with arterial proteoglycans.

METHODS

Mice and diets

The apoB-100-only $Ldlr^{-/-}$ mouse (75% C57Bl/6, 25% 129S/Sv) (16) used in this study was a gift from Dr. Steven Young. Two mouse lines on the apoB-100-only LDL receptor-deficient background were compared for these studies; apoB-100-only $Ldlr^{-/-}$, $Soat2^{+/+}$ and apoB-100-only $Ldlr^{-/-}$, $Soat2^{-/-}$, which were generated as previously described (8). Littermate controls were used to account for genetic heterogeneity. At about 6 weeks of age, mice were switched from a rodent chow diet to one of two semipurified diets consisting of 10% energy as fat with 0.02% cholesterol (wet weight) enriched in either *cis*-MUFAs (55% of total FAs) or long-chain n-3 PUFAs (20% of total FAs). Details of the dietary ingredients and FA compositions have been previously described (8). All experimental animals were euthanized between 10 and 16 weeks of diet treatment. Various endpoints were assessed during this period at the time points indicated. While the plasma cholesterol concentrations and atherosclerosis extent both tend to rise with time of diet exposure, the mice used for LDL binding studies were also evaluated for atherosclerosis extent so that direct comparisons could be made. Mice were maintained in an American Association for Accreditation of Laboratory Animal Care-approved pathogen-free animal facility, and the institutional Animal Care and Use Committee at Wake Forest University Health Sciences approved all experimental protocols.

Plasma lipid and lipoprotein distribution

Blood was taken from each mouse at the terminal time point via heart puncture and transferred to tubes containing 10 μl of protease inhibitor cocktail (Sigma P2714) in 5% Azide and 5% EDTA, and lipids and lipoproteins were measured. Plasma was separated from red blood cells by centrifugation at 7,500 *g* for 15 min at 4°C. Total plasma cholesterol (TPC) concentrations were determined by enzymatic assay as described previously (17, 18). Cholesterol distribution among lipoprotein classes was determined after an aliquot of whole plasma was fractionated by gel filtration chromatography using a Superose-6 10/30 column (GE Healthcare) run at a flow rate of 0.5 ml/min as previously described (15).

LDL isolation

It has previously been reported that isolation of LDL particles by density gradient ultracentrifugation (UC) can dissociate minor apolipoproteins from the particle surface, which could play a role in binding to arterial proteoglycans (19). Thus, a majority of the binding experiments used LDL particles isolated chromatographically as previously described (8).

A Superose 6 10/30 column was equilibrated with sample buffer (100 mM HEPES, 20 mM NaCl, 2 mM $MgCl_2$, 2 mM $CaCl_2$, pH 7.4) containing 50 μl of protease inhibitor (Sigma P8340) per liter of buffer. For LDL isolation, 350 μl of plasma diluted 1:1 with PBS was injected onto the column, and fractions were eluted at a flow rate of 0.4 ml/min. For LDL binding assays, a narrow center of the peak window (23–28 min) was collected and pooled. For LDL compositional analysis, the entire window corresponding to the LDL peak was collected and pooled. After collection, LDLs were maintained at 4°C until analysis.

For comparison, subsets of LDL were also isolated between densities of 1.019 and 1.063 g/ml by ultracentrifugation from pooled plasma (n = 3 mice per group) of all four experimental groups, as previously described (20). All centrifugation steps were performed at room temperature (RT) and the floated LDL was stored at either RT or 4°C until experimental use.

Recombinant BGN isolation

Recombinant BGN was produced using a stable transfected 293-EBNA cell line at LifeCell Corporation. The cell line was created by transferring a BGN polyhistidine fusion construct, originally created for expression using a vaccinia virus expression system (21), into the pCEP4 (Invitrogen Corporation; Carlsbad, CA) expression vector. The resulting plasmid was transfected into 293-EBNA cells and stable-expressing cells selected by culturing in the presence of hygromycin B. Following amplification, cells were seeded into a Celligen Plus bioreactor (New Brunswick Scientific; Edison, NJ) containing 100 g Fibra-Cel disks and grown to saturation. Protein production was initiated by replacing the culture media with serum-free DMEM. Conditioned media was collected every 48 h, with fresh media added back to the bioreactor. Following concentration of the conditioned media using a Pellicon 2 tangential flow system (Millipore Corporation; Bedford, MA), recombinant biglycan was purified using nickel chelating chromatography and elution with a gradient of 0–250 mM imidazole in 20 mM Tris-HCl, 500 mM NaCl, 0.2% CHAPS, pH 8.0. Protein core that had not been well glycosylated was subsequently separated from proteoglycan following anion exchange chromatography on Q-Sepharose and elution with a linear gradient of 0.15–2 M NaCl in PBS, 0.2% CHAPS. Using Coomassie staining, there was no detectable unglycosylated core protein remaining in the proteoglycan preparation as seen after polyacrylamide gel electrophoresis.

LDL-BGN interaction

A Biacore T100 SPR platform (22, 23) was used to quantify the interaction of LDL with immobilized BGN. In the first step, the dextran surfaces of a CM5 biosensor chip (Biacore, Inc.; Piscataway, NJ), for both reference and sample channels, were activated for amine coupling (22). Following surface activation, an antigen affinity-purified polyclonal goat IgG, specific to BGN core protein (R and D Systems; AF2667), was covalently coupled to the dextran surface of the chip through its lysine residues, reproducibly yielding a sparse IgG monolayer in both channels

(sample channel, 14,464 ± 1,606 response unit (RU); reference channel, 11,643 ± 2,720 RU; n = 5). Ethanolamine treatment was then used to block any unreacted sites on the chip surface.

Following mAb immobilization, the system was equilibrated with sample buffer. Each binding cycle began with the delivery of recombinant human BGN (24–27), which had been purified by ion exchange chromatography as described above and kindly provided by Dr. Rick Owens (LifeCell Corporation; Branchburg, NJ). The BGN was added to the sample channel at a concentration of 34 μg/ml protein at a flow rate of 20 μl/min for 180 s followed by a 300 s stabilization period to achieve ~10% saturation of the mAb sample channel surface (1,239 ± 18 RU, n = 30) (see supplementary Fig. IA). BGN capture was quite stable, with an average RU loss of only 3.6 ± 0.9% over 1,700 s. Immunocapturing BGN through its protein core increases the exposure of its GAG chains to enable LDL binding.

After BGN immobilization, various LDL particles were delivered in sample buffer at a flow rate of 30 μl/min for 700 s (binding) to both the reference (mAb only) and sample channels (mAb-BGN), followed by sample buffer at the same rate for 1,000 s (dissociation) (see supplementary Fig. IB). After the binding interaction, 3 M sodium thiocynate was delivered at a flow rate of 30 μl/min to remove the LDL:BGN complex, yielding a fresh mAb surface (Residual RU after each wash = −1 ± −1, n = 6). The biosensor surface was then equilibrated for 300 s with sample buffer prior to the next cycle of BGN capture, LDL binding, and regeneration.

A majority of the binding assays were performed using LDL isolated from whole plasma by HPLC. LDLs were maintained at 10°C in the SPR sample compartment, and data were collected at 25°C. Importantly, binding experiments were performed with fresh LDL (within 24 h of preparation of plasma) to avoid any potential loss in binding signal over time (see supplementary Fig. II). Binding kinetics and concentration curves (0–40 μg/ml LDL cholesterol) for LDL isolated from pooled plasma samples (n = 3 mice/pool) can be found in Fig. 2. All remaining binding experiments were performed on LDL from individual mice at a concentration of 30 μg/ml of LDL cholesterol.

To ensure that CE composition-related differences in binding were not influenced by extraneous proteins coeluting with the LDL particles isolated by HPLC, comparator binding assays were also performed on LDL isolated by UC. Because particle storage temperature and binding temperature also could affect LDL binding, particles isolated and stored at RT were maintained at 25°C in the sample compartment, and data were collected at either 37°C or 25°C (see supplementary Fig. IIIA, B). Particles were also stored at 4°C and maintained in the sample compartment at 10°C, and binding data were collected at 25°C (see supplementary Fig. IIIC for comparison).

LDL particle composition

LDL particle size was determined using size exclusion chromatography with concomitant dynamic light scattering (DLS). After LDL particle isolation, 150 μl of the LDL was injected onto the Superose 6 column and eluted with sample buffer at a flow rate of 0.4 ml/min. Detection was performed at a wavelength of 661 nm by refractive index detector model Optilab rEX (Wyatt Technology) and MALS detector model DAWN HELEOS II (Wyatt Technology). Signals from the detectors were processed using ASTRA software, version 6.0.1.10 (Wyatt Technology), and the hydrodynamic radius was evaluated at the peak of the size distribution curve, generated as a function of particle retention time.

Chemical compositions of the isolated LDLs were determined with enzymatic assays for total cholesterol (TC), free cholesterol (FC), triglyceride (TG), and phospholipid (PL) (TC by Pointe Scientific, Inc.; FC, TG, and PL by Wako Chemicals USA). Total CE mass was calculated for individual LDLs by subtracting the FC from the TC and then multiplying by 1.67 to account for the mass of the acyl chain. LDL CEs were detected and quantified by mass spectrometry as previously described (28). For CE composition analyses, 10 μl of the LDL isolated by HPLC was stored at −80°C under argon to prevent oxidation prior to analysis. At the time of analysis, samples were thawed and diluted in 1 ml of methanol solution containing 500 pg/μl of 17:0 CE as the internal standard and 1 ng/μl of sodium formate. CEs were measured using a Quattro II mass spectrometer equipped with a Z-spray interface (capillary voltage = 3.2 kV; cone voltage = 50 V; source temperature = −80°C; desolvation temperature = 200°C). Samples were maintained at 15°C in a temperature-controlled Spark Holland Reliance autosampler/stacker until analysis. Twenty-five microliters of each sample was infused into the mass spectrometer at 10 μl/min. CEs were quantified in the positive-ion mode by monitoring the common neutral loss of 368.5 Da. The CE molar concentrations were calculated from individual profiles (see supplementary Fig. IV) and the internal standard. Individual CE measurements are reported as percentages of total CE mass.

Protein was measured by the method of Lowry et al. (29) on the ultracentrifuge-isolated LDL. Estimates of the protein for the column-isolated LDL were extrapolated by using the TC:PRO ratio of the centrifugally isolated LDL preparations. Data for the LDL chemical compositions are expressed as a percentage of the total lipid plus protein mass.

Quantification of atherosclerosis

Aortic atherosclerosis was evaluated using both en face and chemical techniques. At the time of necropsy, aortas were removed from mice and preserved in 10% neutral buffered formalin. After a minimum of 24 h fixation, all extraneous tissue and arterial branches were removed from the aorta. In a subset of three mice per experimental group, the aorta was opened longitudinally, pinned flat, and photographed with an mm marker on the photo. After the image was grabbed using Image J software, the entire surface of the aorta and each lesion area were digitized using a digitizing tablet interfaced to a computer using the mm marker as a correction factor. Lesion areas were defined as raised opaque areas on the aortic surface. The percent surface area with lesions was calculated as a simple ratio of aortic lesion area to aorta total surface area. In aortae from all animals, including those used for surface measurements, lipids were extracted in 2:1 chloroform-methanol in a test tube containing a known amount of 5α-cholestane as an internal standard. TC and FC (the latter after saponification) were determined by gas-liquid chromatography, and aortic CE concentration was calculated. The correlation between aortic CE concentrations and surface area occupied by lesion was consistently $r \geq 0.9$ in this and other experiments (see supplementary Fig. V).

Statistical analysis

All statistical analyses were conducted using JMP Software (version 5.0.1.2; Cary, NC). Two-way analysis of variance was used for analyses in which two independent variables were compared, and statistical significance is indicated where observed. Relationships between binding and disease parameters were analyzed by regression analysis and least-squares best-fit regression lines; regression coefficients are included in those figures.

RESULTS

Plasma and lipoprotein cholesterol

The data shown in **Fig. 1** are from mice of each diet and genotype group as measured after 11 weeks of diet

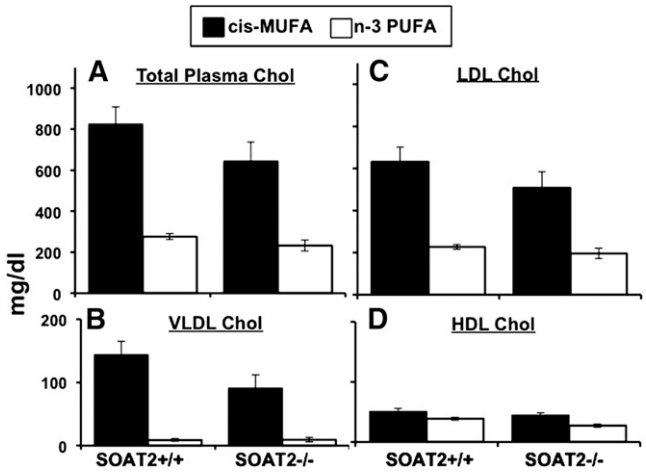

Fig. 1. Effects of dietary FA and SOAT2 status on plasma cholesterol distribution in apoB-100-only, *Ldlr*$^{-/-}$ mice. After 11 weeks of diet induction, blood was collected, EDTA plasma was isolated, and TPC concentrations (A) were determined by enzymatic assay. Cholesterol distribution among lipoprotein classes (B–D) was measured after gel filtration chromatography for separation of lipoprotein classes. The bars represent the means (± SEM) for 11–12 mice for each diet/genotype. For TPC, VLDL, and LDL cholesterol by two-way ANOVA, the values were significantly lower ($P < 0.0001$) for the n-3 PUFA groups, but the *Soat2* genotype groups were not significantly different. No significant interaction effect was found. For HDL cholesterol by two-way ANOVA; values were lower for n-3 PUFA groups and for *Soat2*$^{-/-}$ groups, but no significant interaction was found.

exposure. Two-way ANOVA was used to identify statistically significant differences. In apoB-100-only *Ldlr*$^{-/-}$ mice, consumption of a diet containing n-3 PUFA limited diet-induced hypercholesterolemia compared with mice fed the *cis*-MUFA diet (Fig. 1A). No significant difference in TPC between *Soat2*$^{+/+}$ versus *Soat2*$^{-/-}$ mice was seen. Cholesterol distributions among the lipoprotein classes showed that the increase in TPC levels observed in the *cis*-MUFA-fed mice was a result of significant elevations in cholesterol of both VLDL and LDL, with LDLc comprising about 80% of the total cholesterol pool in both *Soat2* $^{+/+}$ and *Soat2* $^{-/-}$ mice (Fig. 1B,C). No significant difference between *Soat2* genotypes was seen for either VLDL or LDL cholesterol concentrations by two-way ANOVA. For HDL cholesterol, both dietary FA ($P = 0.0008$) and *Soat2* genotype ($P = 0.03$) effects were found to be significant by two-way ANOVA.

LDL composition

Percentage compositions of LDL particles isolated by HPLC from individual mice are shown in **Table 1**. The primary differences in lipid components were limited to the core lipids, i.e., CE and TG. Compared with LDL of *Soat2*$^{+/+}$ mice, LDL particles produced by the *Soat2*$^{-/-}$ mice contained lower percentages of CE and higher percentages of TG, and these differences appeared to be independent of diet. The combined proportions of surface constituents (FC, PL, plus PRO) versus core lipids (CE plus TG) were similar for all groups, and particle diameters, obtained by DLS, showed only a small range of sizes among the particles (23–26 nm). *Soat2*$^{+/+}$ mice consuming the *cis*-MUFA diet had slightly larger LDL particles compared with the other experimental groups.

Individual CE compositions of LDL were quantified by mass spectrometry, and percentages based on FA components are shown in **Table 2**. Dietary fat type and *Soat2* deletion significantly altered the CE species of the LDL particle core. The rank order of monounsaturated fat content of the CE in LDLs isolated from the experimental groups was: *Soat2*$^{+/+}$ fed the *cis*-MUFA (45%) > *Soat2*$^{+/+}$ fed the n-3 PUFA (31%) > *Soat2*$^{-/-}$ fed the *cis*-MUFA (19%) > *Soat2*$^{-/-}$ mice fed the n-3 PUFA (11%). *Soat2*$^{-/-}$ mice fed *cis*-MUFA and n-3 PUFA had CEs that consisted primarily of n-6 PUFAs (64% and 56%, respectively). In contrast, the percentage of CEs consisting of the n-6 polyunsaturated fat in *Soat2*$^{+/+}$ mice fed *cis*-MUFA and n-3 PUFA were 40% and 17%, respectively. In sum, LDL cholesterol ester composition was highly sensitive to both SOAT2 status and dietary fat composition.

In summary, mice consuming the *cis*-MUFA diet had the highest LDL cholesterol concentrations, although no significant differences between the *Soat2*$^{+/+}$ and *Soat2*$^{-/-}$ mice were observed. The percentage of LDL total mass that was monounsaturated CE was 19.5% in *Soat2*$^{+/+}$ mice consuming the *cis*-MUFA diet and was 12.7% in *Soat2*$^{+/+}$ mice fed the n-3 PUFA diet. In contrast, *Soat2*$^{-/-}$ mice consuming the *cis*-MFUA diet had 6.25% of LDL mass as monounsaturated CE, whereas *Soat2*$^{-/-}$ mice had LDL particles with only 3.85% of mass as monounsaturated CE.

LDL binding to biglycan

LDL binding to human BGN was measured using SPR by delivering LDL particles isolated from mice to immunocaptured human BGN, the core protein of which shares

TABLE 1. Effect of diet and *Soat2* deletion on LDL particle composition

		Percentage *wt/wt*					
Genotype	Diet	FC	CE	TG	PL	PRO	Diameter (nm)
Soat2$^{+/+}$	*cis*- MUFA	10.8 (0.4)	43.0 (1.0)	1.9 (0.5)	25.8 (2.0)	18.6 (0.5)	25.0 (0.3)
Soat2$^{+/+}$	n-3 PUFA	11.9 (0.3)	41.6 (0.9)	2.8 (0.8)	23.6 (1.6)	20.1 (0.4)	24.0 (0.4)
Soat2$^{-/-}$	*cis*- MUFA	10.9 (0.3)	34.1 (0.7)	10.3 (0.5)	21.2 (0.7)	23.7 (0.3)	23.9 (0.6)
Soat2$^{-/-}$	n-3 PUFA	11.8 (0.6)	34.5 (1.7)	8.7 (1.2)	27.2 (3.3)	17.7 (0.8)	23.2 (0.4)
Two-way ANOVA							
Diet effect		$P = 0.02$	ns	ns	ns	ns	$P = 0.008$
Genotype effect		ns	$P < 0.0001$	$P < 0.0001$	ns	ns	$P = 0.004$
Interaction effect		ns	ns	ns	ns	$P = 0.0003$	ns

LDL diameter was determined using DLS. All values represent the means (± SEM) for 15–17 mice for each diet/genotype group.

TABLE 2. Individual cholesteryl esters of LDL

Genotype	Diet	Cholesteryl Esters *wt* %								
		16:0	18:0	16:1	18:1	18:2	20:4	18:3	20:5	22:6
Soat2$^{+/+}$	*cis*-MUFA	5.5 (0.3)	1.2 (0.2)	9.9 (0.4)	35.3 (2.6)	13.2 (0.7)	27.1 (2.3)	0.8 (0.1)	1.9 (0.2)	5.1 (0.4)
Soat2$^{+/+}$	n-3 PUFA	6.2 (0.3)	1.2 (0.2)	14.0 (0.7)	16.5 (0.5)	7.4 (0.4)	10.0 (0.4)	1.2 (0.1)	33.6 (1.1)	10.0 (0.3)
Soat2$^{-/-}$	*cis*-MUFA	3.7 (0.5)	0.8 (0.2)	5.2 (0.7)	13.2 (3.6)	19.1 (1.2)	44.6 (3.5)	1.0 (0.1)	3.5 (0.5)	8.9 (0.7)
Soat2$^{-/-}$	n-3 PUFA	3.4 (0.3)	0.5 (0.1)	5.7 (0.2)	5.5 (0.5)	10.7 (0.4)	16.7 (0.6)	1.0 (0.1)	42.3 (1.5)	14.2 (0.5)
Two-way ANOVA										
Diet effect		ns	ns	$P < 0.0001$	$P < 0.0001$	$P < 0.0001$	$P < 0.0001$	$P = 0.003$	$P < 0.0001$	$P < 0.0001$
Genotype effect		$P = 0.0001$	$P = 0.001$	$P < 0.0001$	$P < 0.0001$	$P < 0.0001$	$P < 0.0001$	ns	$P < 0.0001$	$P < 0.0001$
Interaction effect		ns	ns	$P = 0.002$	$P = 0.02$	ns	$P = 0.02$	$P = 0.004$	$P = 0.0002$	ns

Cholesteryl esters are expressed as a percentage of the total CE of the LDL as determined by mass spectrometry. All values represent the means (± SEM) for 13–19 mice for each diet/genotype.

98% amino acid homology with mouse biglycan (30). As illustrated in **Fig. 2A**, each experiment consisted of a 700 s binding step as LDL isolated from pooled plasma samples from *Soat2*$^{+/+}$ mice consuming the *cis*-MUFA diet (n = 3 mice/pool, 0–40 μg/ml LDL cholesterol) flowed over the immunoabsorbed BGN; this period was followed by a 1,000 s dissociation step as sample buffer was delivered to the chip. Each RU versus time trace has been corrected for nonspecific binding by subtracting the RU from the reference channel (which contained antibody alone) from the LDL binding signals from the sample channel that contained immunocaptured BGN. A comparison of data across experiments was facilitated by normalizing each peak and predissociation LDL RU value by the signal resulting from BGN immunocapture (RU). LDL binding at the peak responses are plotted as a function of LDL cholesterol concentration and fitted to a one-site binding model for particles isolated from pooled plasma from each experimental group shown in Fig. 2B. Using SigmaPlot 11.0, the K_d and B_{max} were calculated for all experimental groups, and the values represent LDL from the *Soat2*$^{+/+}$ mice consuming the *cis*-MUFA diet and the average of the LDL from the remaining three experimental groups, inasmuch as the curves for the latter were essentially superimposable. LDL cholesterol (23.3 μg/ml) was required from the *Soat2*$^{+/+}$ group consuming the *cis*-MUFA diet to bind to half the proteoglycan sites at equilibrium (K_d). In comparison, the other three experimental groups required 3-fold higher concentrations of LDL cholesterol (68 μg/ml) to achieve the same amount of binding. Additionally, B_{max}, the ratio of LDL binding RU to BGN-captured RU for the LDL from the *Soat2*$^{+/+}$ mice consuming the *cis*-MUFA diet, was also higher compared with the other experimental groups (1.66 versus 1.35).

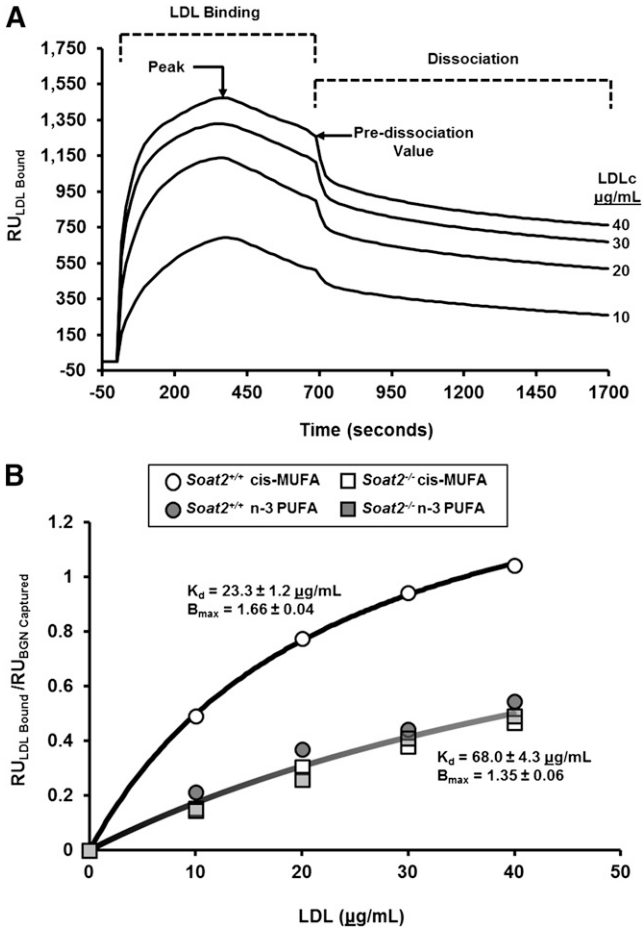

Fig. 2. Interaction of LDL isolated from pooled plasma of apoB-100-only *Ldlr*$^{-/-}$ mice with immobilized biglycan. A: Kinetic responses with different concentrations of LDLc (0–40 μg/ml) isolated from pooled plasma samples (n = 3) from *Soat2*$^{+/+}$ mice consuming the *cis*-MUFA diet. B: LDL peak binding response normalized to BGN response for different concentrations of LDLc (0–40 μg/ml) isolated from pooled plasma samples in all experimental groups (n = 3 mice/group).

LDL binding to BGN was also measured using LDL particles isolated from plasma of individual mice at a concentration of 30 μg/ml of LDL cholesterol. LDL of *Soat2*$^{+/+}$ mice consuming the *cis*-MUFA diet had the highest affinity to BGN, as illustrated by the prompt, large signal changes (RU) presented in **Fig. 3A**, top trace. LDL particles isolated from individual *Soat2*$^{+/+}$ mice consuming the n-3 PUFA diet exhibited about a 2-fold reduction in binding affinity in this experiment. Even greater signal reductions were observed with LDL particles isolated from *Soat2*$^{-/-}$ mice fed the *cis*-MUFA and the n-3 PUFA diets, as illustrated by the kinetic traces shown in Fig. 3A. Incubating LDL particles with excess chondroitin sulfate (CS) GAGs to block potential binding sites reduced the RU signals essentially to baseline (Fig. 3A, bottom trace), confirming the specificity of LDL:BGN binding.

LDL from all experimental mice resulted in a rapid rise in RU during the initial ~300 s of the binding phase.

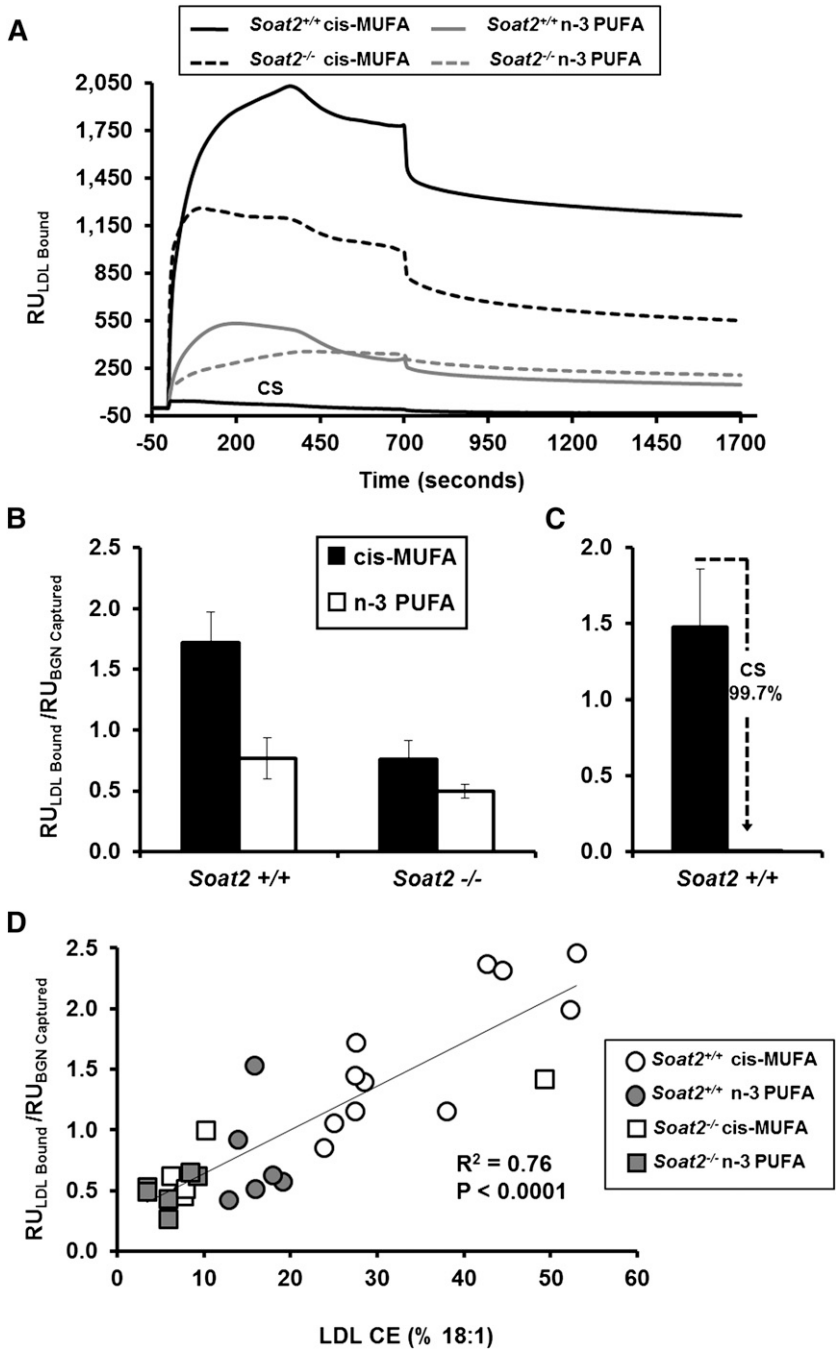

Fig. 3. Interaction of LDL isolated from plasma of individual apoB-100-only $Ldlr^{-/-}$ mice with immobilized biglycan as assessed by SPR. Binding was determined using 30 μg/ml of LDLc isolated from plasma of individual mice. A: Representative kinetic plots of LDL binding for a representative mouse LDL sample from each experimental group. CS shows chondroitin sulfate inhibition of LDL binding where LDL from a $Soat2^{+/+}$ mouse consuming the *cis*-MUFA diet was studied. B: Peak binding responses of LDL particles. The bars represent the means (± SEM) for 6–12 mice for each diet/genotype group; for all groups of mice, diet was fed for 12 weeks at the time of blood sampling. By two-way ANOVA, the diet effect was significant ($P = 0.0006$), and the responses for $Soat2^{+/+}$ versus $Soat2^{-/-}$ groups were significantly different ($P = 0.005$), but there was no significant interaction. C: Binding of LDL particles isolated from $Soat2^{+/+}$ mice consuming the *cis*-MUFA diet incubated with or without 25 μg/ml of CS GAGs. D: Regression analysis comparing LDL binding to immobilized BGN with the percentage of CO in the CE of the different LDL particles. The line is the least-squares best-fit regression line, and the regression coefficient was highly significant.

Kinetic analyses for the various study groups yielded comparable although sometimes variable half-times that were not apparenty related to the relative RU response. Peak RU signals were typically followed by a small drop in RU as LDL delivery continued out to 700 s. For example, the ratio of the peak to predissociation RU signals averaged 1.34 ± 0.14 (n = 6) for LDL particles from $Soat2^{+/+}$ mice consuming the *cis*-MUFA diet. Buffer delivery reduced the RU signals even

further, to 0.48 ± 0.18 (n = 6) times the peak values for this group. The decreases in binding from the predissociation point during the buffer wash phase remained proportional for each experimental group. The reduction in RU signals may reflect the transient binding of metastable LDL aggregates that form and dissociate quickly from the immunocaptured biglycan. Alternatively, changes within the secondary structure of the biglycan may occur as a consequence of the LDL binding, limiting the available charged sequences. Interestingly, it has been reported that GAG chains present on proteoglycans can self–associate, and thus it is possible that after the initial interaction with LDL particles, the GAGs present on the biglycan may undergo a small conformational change. Such a change could not only result in the release of minor amounts of bound LDL particles but could also render previously accessible regions of the GAG chain inaccessible (31).

Results of the normalized peak analysis at the maximum response value for LDL of each combination of diet and genotype are presented as averaged data in bar graph format in Fig. 3B. Consistent with the data for LDL isolated from the pooled plasma (Fig. 2A), LDL particles isolated from individual *Soat2*$^{+/+}$ mice consuming the *cis*-MUFA diet had the highest affinity for BGN. Statistically significant differences in binding between diet and genotype groups were maintained when a similar analysis was applied to the predissociation binding signals (data not shown). Incubating LDL with CS successfully inhibited the LDL:BGN interaction with almost complete inhibition (>99%, n = 6) achieved by incubating with 25 μg/ml CS (Fig. 3C). Regression analysis was performed to investigate the relationship between the extent of LDL-biglycan binding and CE composition of LDL (Fig. 3D), and results revealed a highly significant positive association (R^2 = 0.76, P < 0.0001) between the percentage of CO in the LDL CE and the affinity of the LDL particle for BGN.

Atherosclerosis

Finally, by quantifying the amount of CE deposited in the aorta during diet induction, the extent of atherosclerosis was evaluated in 21 individual LDL donor mice for which LDL BGN binding was also measured in terminal blood samples. Mice consuming dietary n-3 PUFA and mice with *Soat2* gene deletions consistently had lower aortic CE levels compared with *Soat2*$^{+/+}$ mice consuming the *cis*-MUFA diet (**Fig. 4A**). Regression analysis was performed to investigate relationships between atherosclerosis extent and both the percentage of LDL CE as CO and LDL BGN binding (Fig. 4B, C). Results showed highly significant positive relationships between the extent of atherosclerosis and both the percentage of CE as CO in the core of the particle (R^2 = 0.53 P = 0.0003, Fig. 4B) and the LDL binding response to BGN (R^2 = 0.49 P = 0.0008, Fig. 4C).

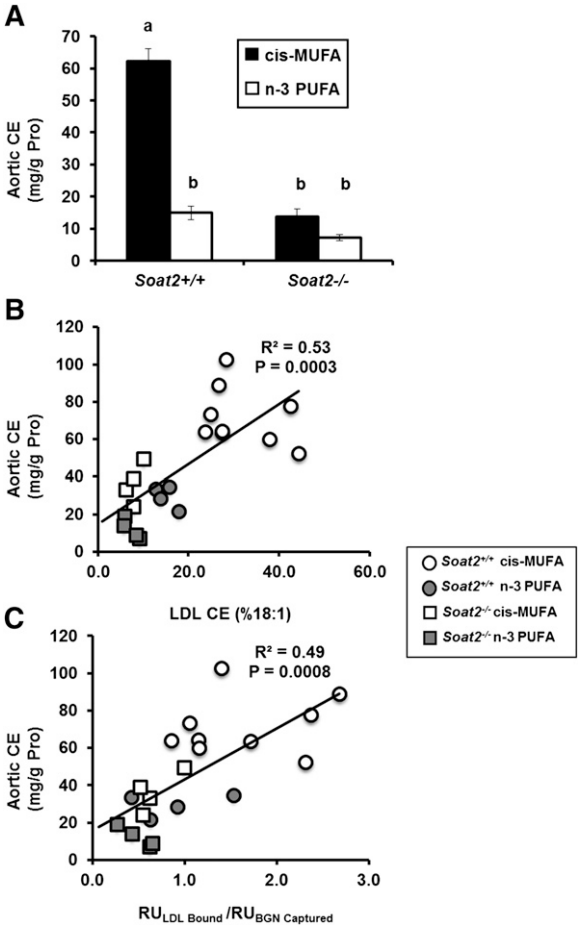

Fig. 4. Atherosclerosis and its relationship to LDL CO and LDL-BGN binding. A: CE concentration of the aorta (a measure of atherosclerosis extent) for *Soat2*$^{+/+}$ and *Soat2*$^{-/-}$ mice fed the *cis*-MUFA or n-3 PUFA diet for an average of 15 weeks. The bars represent the means (± SEM) for 20–30 mice for each experimental group. Two-way ANOVA showed significant differences by diet FA (P < 0.0001) and *Soat2* genotype (P < 0.0001) with a significant interaction (P < 0.0001). Significant differences are indicated with a post hoc analysis using Tukey's honestly significant difference test. For B and C, regression analyses comparing atherosclerosis extent after 12.4 to13.5 weeks of diet induction in 21 different mice in each of the four diet groups, with B: the percentage of CO in the CE of the LDL particle core and C: the SPR response of LDL binding to BGN. The lines are the least-squares best-fit regression lines and show statistically significant associations of the properties of LDL with atherosclerosis extent.

DISCUSSION

The principal finding of this study in a mouse model of atherosclerosis, the apoB-100-only *Ldlr*$^{-/-}$ mouse, is that dietary changes and genetic manipulations that enrich the LDL particle core in CO promoted atherosclerosis and increased the affinity for LDL binding to the specific proteoglycan, biglycan, as quantified by a novel SPR method. Our approach provides real-time measurements of the rate and extent of formation and dissociation of LDL:BGN complexes, with a sensitivity comparable to solid-phase binding measurements that yield only affinity data (4). The primary compositional difference between LDL particles isolated from the *Soat2*$^{+/+}$ mice consuming the *cis*-MUFA diet and those from the other experimental groups is the abundance of monounsaturated CE packaged into the particle core. Regression analysis revealed strong and

highly significant correlations between the proportions of CE as CO in the LDL particle and the affinity for the immobilized BGN. Additionally, there was a strong relationship between LDL binding and the degree of atherosclerosis that developed. These results indicate that SOAT2-derived CE containing monounsaturated FAs in the core of LDL may result in a prolonged residence time of LDL in the artery wall that could lead to accelerated development of atherosclerosis. These findings are in agreement with previous studies showing that dietary consumption of n-3 PUFAs by nonhuman primates resulted in the production of LDL particles with a decreased affinity for proteoglycans compared with their lard-fed counterparts (32–34).

This study also helps address a number of paradoxical questions that remain unanswered as to what factors appear to be more important in the development of atherosclerosis. Our report indicates that LDL particle composition is a critical factor driving atherogenesis. This becomes apparent when considering that there were no significant differences in plasma lipoprotein cholesterol concentrations between the *Soat2*$^{+/+}$ and *Soat2*$^{-/-}$ mice consuming the *cis*-MUFA diet; in contrast, the *Soat2*$^{-/-}$ mice had significantly less CO in the particle core, which had been replaced with TG and CE containing n-6 polyunsaturated FAs, the latter presumably being derived from the plasma enzyme lecithin:cholesterol acyltransferase. At the same time, a large attenuation in the development of atherosclerosis was seen. This is an important observation when considering that monounsaturated fats such as olive oil are still being promoted as healthy and protective against heart disease (35–37). Additionally, several reports suggest that LDL particles enriched in polyunsaturated fats are more susceptible to oxidation (38, 39), a process thought to promote the development of atherosclerosis. Although this remains possible, our data demonstrate that packaging of the polyunsaturated FAs (n-3 or n-6) into the LDL core CE results in a reduced affinity of LDL particles for arterial proteoglycans. Thus, while being more susceptible to oxidation, such LDLs would probably have a shortened residence time in the artery wall, which may have the effect of limiting the oxidative modifications that can take place.

We used LDL isolated by gel filtration chromatography for the binding assays so that we did not modify the surface components, as might occur during ultracentrifugation. The LDL particles used in the binding assay were only in the narrow center cut from the LDL peak off the superose column. Necessarily, for compositional analyses, material from the entire column peak was analyzed, so it is possible that small differences in composition between the LDL used in the binding assay and the LDL analyzed for composition could have been present.

While a molecular mechanism directly responsible for the increased binding of CO-enriched LDL particles is not presented in this report, we postulate that the differences seen in this study are primarily a result of conformational differences in apoB-100 on the LDL particle surface. ApoB-100 contains several proteoglycan binding sites (40, 41), and the structure of apoB-100 on the LDL particle surface has been shown to be sensitive to both temperature and deviations in the organization of the neutral lipid core (42). The physical state of the LDL particle core is dependent upon fatty acyl composition, and it has been shown that the presence of more-saturated and monounsaturated FAs results in a more-liquid-crystalline (anisotropic) particle core, whereas a shift to more polyunsaturated FAs results in a more-liquid (isotropic) core. Thus, it seems reasonable that the LDL particles enriched with CE containing saturated and monounsaturated FAs would have an anisotropic core that could lead to a modified apoB-100 conformation where it extends farther outside of the PL monolayer (43), for example. We speculate that this could result in an LDL particle with more proteoglycan binding sites exposed on the particle surface, which act cooperatively to increase interactions with proteoglycans. The consequent result could be increased LDL retention in the arterial intima and more atherosclerosis.

The authors thank Dr. Rick Owens (LifeCell Corporation, Branchburg, NJ) for providing the recombinant human biglycan used in this study. We acknowledge the mass spectrometry core lab run by Dr. Michael Thomas and Mike Samuels (Wake Forest School of Medicine, Biochemistry Department) for performing the mass spectrometry analyses on the LDL particle cholesteryl esters. Thanks to Mary C. Stahle for her expert technical assistance with the SPR measurements.

REFERENCES

1. Roger, V. L., A. S. Go, D. M. Lloyd-Jones, E. J. Benjamin, J. D. Berry, W. B. Borden, D. M. Bravata, S. Dai, E. S. Ford, C. S. Fox, et al. 2012. Heart disease and stroke statistics–2012 update: a report from the American Heart Association. *Circulation.* **125:** e1002.
2. Williams, K. J., and I. Tabas. 1995. The response-to-retention hypothesis of early atherogenesis. *Arterioscler. Thromb. Vasc. Biol.* **15:** 551–561.
3. Camejo, G. 1982. The interaction of lipids and lipoproteins with the intercellular matrix of arterial tissue: its possible role in atherogenesis. *Adv. Lipid Res.* **19:** 1–53.
4. Skålén, K., M. Gustafsson, E. K. Rydberg, L. M. Hulten, O. Wiklund, T. L. Innerarity, and J. Boren. 2002. Subendothelial retention of atherogenic lipoproteins in early atherosclerosis. *Nature.* **417:** 750–754.
5. O'Brien, K. D., K. L. Olin, C. E. Alpers, W. Chiu, M. Ferguson, K. Hudkins, T. N. Wight, and A. Chait. 1998. Comparison of apolipoprotein and proteoglycan deposits in human coronary atherosclerotic plaques: colocalization of biglycan with apolipoproteins. *Circulation.* **98:** 519–527.
6. Zeng, X., J. Chen, Y. I. Miller, K. Javaherian, and K. S. Moulton. 2005. Endostatin binds biglycan and LDL and interferes with LDL retention to the subendothelial matrix during atherosclerosis. *J. Lipid Res.* **46:** 1849–1859.
7. Kunjathoor, V. V., D. S. Chiu, K. D. O'Brien, and R. C. LeBoeuf. 2002. Accumulation of biglycan and perlecan, but not versican, in lesions of murine models of atherosclerosis. *Arterioscler. Thromb. Vasc. Biol.* **22:** 462–468.
8. Bell III, T. A., K. Kelley, M. D. Wilson, J. K. Sawyer, and L. L. Rudel. 2007. Dietary fat-induced alterations in atherosclerosis are abolished by ACAT2-deficiency in ApoB100 only, *LDLr*$^{-/-}$ mice. *Arterioscler. Thromb. Vasc. Biol.* **27:** 1396–1402.
9. Rudel, L. L., M. G. Bond, and B. C. Bullock. 1985. LDL heterogeneity and atherosclerosis in nonhuman primates. *Ann. N. Y. Acad. Sci.* **454:** 248–253.
10. Rudel, L. L., F. L. Johnson, J. K. Sawyer, M. S. Wilson, and J. S. Parks. 1995. Dietary polyunsaturated fat modifies low-density lipoproteins and reduces atherosclerosis of nonhuman primates with high and low diet responsiveness. *Am. J. Clin. Nutr.* **62:** 463S–470S.

11. Rudel, L. L., J. S. Parks, and J. K. Sawyer. 1995. Compared with dietary monounsaturated and saturated fat, polyunsaturated fat protects African green monkeys from coronary artery atherosclerosis. *Arterioscler. Thromb. Vasc. Biol.* **15:** 2101–2110.
12. Reaven, P., S. Parthasarathy, B. J. Grasse, E. Miller, D. Steinberg, and J. L. Witztum. 1993. Effects of oleate-rich and linoleate-rich diets on the susceptibility of low density lipoprotein to oxidative modification in mildly hypercholesterolemic subjects. *J. Clin. Invest.* **91:** 668–676.
13. Ma, J., A. R. Folsom, L. Lewis, and J. H. Eckfeldt. 1997. Relation of plasma phospholipid and cholesterol ester fatty acid composition to carotid artery intima-media thickness: the Atherosclerosis Risk in Communities (ARIC) Study. *Am. J. Clin. Nutr.* **65:** 551–559.
14. Parini, P., M. Davis, A. T. Lada, S. K. Erickson, T. L. Wright, U. Gustafsson, S. Sahlin, C. Einarsson, M. Eriksson, B. Angelin, et al. 2004. ACAT2 is localized to hepatocytes and is the major cholesterol-esterifying enzyme in human liver. *Circulation.* **110:** 2017–2023.
15. Lee, R. G., K. L. Kelley, J. K. Sawyer, R. V. Farese, Jr., J. S. Parks, and L. L. Rudel. 2004. Plasma cholesteryl esters provided by lecithin:cholesterol acyltransferase and acyl-coenzyme a:cholesterol acyltransferase 2 have opposite atherosclerotic potential. *Circ. Res.* **95:** 998–1004.
16. Veniant, M. M., C. H. Zlot, R. L. Walzem, V. Pierotti, R. Driscoll, D. Dichek, J. Herz, and S. G. Young. 1998. Lipoprotein clearance mechanisms in LDL receptor-deficient "Apo-B48-only" and "Apo-B100-only" mice. *J. Clin. Invest.* **102:** 1559–1568.
17. Carr, T. P., C. J. Andresen, and L. L. Rudel. 1993. Enzymatic determination of triglyceride, free cholesterol, and total cholesterol in tissue lipid extracts. *Clin. Biochem.* **26:** 39–42.
18. Temel, R. E., R. G. Lee, K. L. Kelley, M. A. Davis, R. Shah, J. K. Sawyer, M. D. Wilson, and L. L. Rudel. 2005. Intestinal cholesterol absorption is substantially reduced in mice deficient in both ABCA1 and ACAT2. *J. Lipid Res.* **46:** 2423–2431.
19. Stahlman, M., P. Davidsson, I. Kanmert, B. Rosengren, J. Boren, B. Fagerberg, and G. Camejo. 2008. Proteomics and lipids of lipoproteins isolated at low salt concentrations in D2O/sucrose or in KBr. *J. Lipid Res.* **49:** 481–490.
20. Lee, R. G., R. Shah, J. K. Sawyer, R. L. Hamilton, J. S. Parks, and L. L. Rudel. 2005. ACAT2 contributes cholesteryl esters to newly secreted VLDL, whereas LCAT adds cholesteryl ester to LDL in mice. *J. Lipid Res.* **46:** 1205–1212.
21. Hocking, A. M., R. A. Strugnell, P. Ramamurthy, and D. J. McQuillan. 1996. Eukaryotic expression of recombinant biglycan. Post-translational processing and the importance of secondary structure for biological activity. *J. Biol. Chem.* **271:** 19571–19577.
22. Hantgan, R. R., and M. C. Stahle. 2009. Integrin priming dynamics: mechanisms of integrin antagonist-promoted alphaIIbbeta3:PAC-1 molecular recognition. *Biochemistry.* **48:** 8355–8365.
23. Hantgan, R. R., M. C. Stahle, and D. A. Horita. 2008. Entropy drives integrin alphaIIbbeta3:echistatin binding–evidence from surface plasmon resonance spectroscopy. *Biochemistry.* **47:** 2884–2892.
24. Berendsen, A. D., L. W. Fisher, T. M. Kilts, R. T. Owens, P. G. Robey, J. S. Gutkind, and M. F. Young. 2011. Modulation of canonical Wnt signaling by the extracellular matrix component biglycan. *Proc. Natl. Acad. Sci. USA.* **108:** 17022–17027.
25. Groeneveld, T. W., M. Oroszlan, R. T. Owens, M. C. Faber-Krol, A. C. Bakker, G. J. Arlaud, D. J. McQuillan, U. Kishore, M. R. Daha, and A. Roos. 2005. Interactions of the extracellular matrix proteoglycans decorin and biglycan with C1q and collectins. *J. Immunol.* **175:** 4715–4723.
26. Mercado, M. L., A. R. Amenta, H. Hagiwara, M. S. Rafii, B. E. Lechner, R. T. Owens, D. J. McQuillan, S. C. Froehner, and J. R. Fallon. 2006. Biglycan regulates the expression and sarcolemmal localization of dystrobrevin, syntrophin, and nNOS. *FASEB J.* **20:** 1724–1726.
27. Rafii, M. S., H. Hagiwara, M. L. Mercado, N. S. Seo, T. Xu, T. Dugan, R. T. Owens, M. Hook, D. J. McQuillan, M. F. Young, et al. 2006. Biglycan binds to alpha- and gamma-sarcoglycan and regulates their expression during development. *J. Cell. Physiol.* **209:** 439–447.
28. Miller, C. D., M. J. Thomas, B. Hiestand, M. P. Samuel, M. D. Wilson, J. K. Sawyer, and L. L. Rudel. 2012. Cholesteryl esters associated with ACAT2 predict coronary artery disease in patients with symptoms of acute coronary syndrome. *Acad. Emerg. Med.* **19:** 673–682.
29. Lowry, O. H., N. J. Rosebrough, A. L. Farr, and R. J. Randall. 1951. Protein measurement with the Folin phenol reagent. *J. Biol. Chem.* **193:** 265–275.
30. Wegrowski, Y., J. Pillarisetti, K. G. Danielson, S. Suzuki, and R. V. Iozzo. 1995. The murine biglycan: complete cDNA cloning, genomic organization, promoter function, and expression. *Genomics.* **30:** 8–17.
31. Fransson, L. A., and B. Havsmark. 1982. Structural requirements for heparin sulphate self-association. *Carbohydr. Res.* **110:** 135–144.
32. Edwards, I. J., A. K. Gebre, W. D. Wagner, and J. S. Parks. 1991. Reduced proteoglycan binding of low density lipoproteins from monkeys (Macaca fascicularis) fed a fish oil versus lard diet. *Arterioscler. Thromb. Vasc. Biol.* **11:** 1778–1785.
33. Manning, J. M., A. K. Gebre, I. J. Edwards, W. D. Wagner, L. L. Rudel, and J. S. Parks. 1994. Dietary polyunsaturated fat decreases interaction between low density lipoproteins and arterial proteoglycans. *Lipids.* **29:** 635–641.
34. Parks, J. S., A. K. Gebre, I. J. Edwards, and W. D. Wagner. 1991. Role of LDL subfraction heterogeneity in the reduced binding of low density lipoproteins to arterial proteoglycans in cynomolgus monkeys fed a fish oil diet. *J. Lipid Res.* **32:** 2001–2008.
35. Kris-Etherton, P. M. 1999. AHA science advisory: monounsaturated fatty acids and risk of cardiovascular disease. *J. Nutr.* **129:** 2280–2284.
36. Gillingham, L. G., S. Harris-Janz, and P. J. Jones. 2011. Dietary monounsaturated fatty acids are protective against metabolic syndrome and cardiovascular disease risk factors. *Lipids.* **46:** 209–228.
37. Mensink, R. P., and M. B. Katan. 1989. Effect of a diet enriched with monounsaturated or polyunsaturated fatty acids on levels of low-density and high-density lipoprotein cholesterol in healthy women and men. *N. Engl. J. Med.* **321:** 436–441.
38. Hau, M. F., A. H. Smelt, A. J. Bindels, E. J. Sijbrands, A. Van der Laarse, W. Onkenhout, W. van Duyvenvoorde, and H. M. Princen. 1996. Effects of fish oil on oxidation resistance of VLDL in hypertriglyceridemic patients. *Arterioscler. Thromb. Vasc. Biol.* **16:** 1197–1202.
39. Thomas, M. J., T. Thornburg, J. Manning, K. Hooper, and L. L. Rudel. 1994. Fatty acid composition of low-density lipoprotein influences its susceptibility to autoxidation. *Biochemistry.* **33:** 1828–1834.
40. Camejo, G., S. O. Olofsson, F. Lopez, P. Carlsson, and G. Bondjers. 1988. Identification of Apo B-100 segments mediating the interaction of low density lipoproteins with arterial proteoglycans. *Arteriosclerosis.* **8:** 368–377.
41. Hirose, N., D. T. Blankenship, M. A. Krivanek, R. L. Jackson, and A. D. Cardin. 1987. Isolation and characterization of four heparin-binding cyanogen bromide peptides of human plasma apolipoprotein B. *Biochemistry.* **26:** 5505–5512.
42. Weisgraber, K. H., and S. C. Rall, Jr. 1987. Human apolipoprotein B-100 heparin-binding sites. *J. Biol. Chem.* **262:** 11097–11103.
43. Kumar, V., S. J. Butcher, K. Oorni, P. Engelhardt, J. Heikkonen, K. Kaski, M. Ala-Korpela, and P. T. Kovanen. 2011. Three-dimensional cryoEM reconstruction of native LDL particles to 16A resolution at physiological body temperature. *PLoS ONE.* **6:** e18841.